Int. J. Solids Structures Vol. 24, No. 4, pp. 391–416, 1988
Printed in Great Britain.

0020–7683/88 $3.00 + .00

DESCRIPTION OF INELASTIC DEFORMATION AND DEGRADATION OF CONCRETE

M. KLISINSKI and Z. MRÓZ
Institute of Fundamental Technological Research, Warsaw, Poland

(*Received* 12 *May* 1987; *in revised form* 30 *September* 1987)

Abstract—A general constitutive model for concrete is discussed in which the total strain rate is decomposed into elastic, plastic and damage strain rates. The rate equations are formulated for all strain rate portions together with evolution rules for hardening and damage state variables. The coupling effect between damage and plastic deformation is considered by introducing yield and damage surfaces and formulating proper interaction rules. Both axisymmetric and general three-dimensional stress states are considered for which monotonic and cyclic loading conditions are assumed. The model is aimed to describe material behavior for a variety of loading histories. Its applicability is illustrated by considering uniaxial, biaxial and triaxial compression with superposed shear stresses.

1. INTRODUCTION

In numerous cases involving non-conventional design of concrete structures there is a need for more refined inelastic analysis of concrete that takes into account phenomena such as progressive cracking and inelastic deformation. Such incremental analysis is usually required not only to provide an assessment of the failure load but also to predict deformational response and the degree of degradation in states preceding eventual collapse. Tall buildings, offshore oil platforms, nuclear reactor containment structures, and gasification vessels, etc. are examples of such complex structures for which a refined incremental analysis is required.

The inelastic analysis should be based on a properly formulated and sufficiently accurate constitutive model for concrete. Considerable progress has been made during the last two decades in developing constitutive models for concrete and schemes for conducting inelastic analysis of reinforced concrete structures. A comprehensive review of these developments can be found, for instance, in a book by Chen (1982). Concrete has usually been modelled as a non-linear elastic by Cedolin *et al.* (1977), Chen and Chen (1975), Kotsovos and Newman (1978), a hypoelastic by Elwi and Murray (1979), Gerstle (1981), Liu *et al.* (1972), a perfectly plastic or a hardening and softening elastic–plastic material by Mróz (1973), Murray *et al.* (1979), Willam and Warnke (1975). Depending on the type of structural problem, it may be possible to use such simplified constitutive descriptions to simulate structural behaviour with a sufficient degree of accuracy.

However, at present there is no generally accepted constitutive model that could be used with confidence to simulate material response under a variety of loading conditions including both monotonic and cyclic loading. Besides structural applications, such a general model could also be used to describe experimental results obtained for complex stress states and loading histories, thus facilitating understanding and interpretation of the material behaviour.

The present paper is aimed at formulation of a constitutive model that can account for progressive material cracking and irreversible deformation under both monotonic and cyclic non-proportional loading in the pre-critical range. The basic assumptions and the general structure of such a model have been discussed in the earlier paper by Dragon and Mróz (1979), and here we shall develop this formulation further. It will be assumed that internal damage (or cracking) is accompanied by irreversible (or plastic) deformation and the total strain rate is decomposed into elastic, damage (cracking) and plastic portions—for which independent rate equations are formulated. The coupling between damage and

plastic deformation is accounted for by introducing hardening and degradation state variables and proper evolution rules. The discussion of the coupling implications can be found in the paper by Hueckel and Maier (1977). Since viscous effects are neglected thus the strain increments or rates are treated as instantaneous. The extension of the present model to the post-critical range requires incorporation of additional effects in conjunction with a localization of deformation. However, they cannot be described at the material constitutive level.

Related formulations involving elastic–cracking models for concrete have been presented by Dougill (1976), Dougill *et al.* (1977), Krajcinovic and Fonseka (1981), Mazars (1982), and an elastic–plastic–cracking model was discussed by Bazant and Kim (1979).

In Section 2, the basic model assumptions and the structure of the constitutive equations are presented, whereas in Section 3 the model is applied to simulate uniaxial, biaxial and axisymmetric triaxial compression tests. The general three-dimensional formulation is also provided and is used to predict some recent experimental data.

2. FORMULATION OF CONSTITUTIVE MODEL FOR CONCRETE

As described by Dragon and Mróz (1979) the model formulation is based on the assumption that the plastic deformation of concrete and progressive damage (fracturing) may occur simultaneously or separately depending on the stress state. Under monotonic loading the plastic deformation is associated with accumulation of irreversible strain, whereas the damage process is macroscopically manifested as stiffness degradation during unloading. The macroscopic irreversible strain is attributed to micro slips occurring at cracks within the mortar or at the mortar–aggregate interface and also to irreversible opening of cracks under tension. The variation of elastic compliance results from progressive cracking usually occurring in a stable manner before the critical crack density is reached. Although concrete is a composite material, it will be described in terms of total stress and strain states without decomposition into mortar and aggregate states.

The alternative treatment of concrete as a composite material has been presented by Ortiz and Popov (1982a, b), and Ortiz (1985). Whereas such an approach is physically more sound, it eventually results in constitutive relations expressed in terms of total stress and strain components that are regarded as an external action on and a response of the representative element. We therefore use a phenomenological approach and regard stress or strain states as average values over the representative element composed of both mortar and aggregate. The composite character of concrete should be reflected in the selection of proper forms of yield and damage surfaces and also in the evolution rules for the appropriate state variables.

Referring to Figs 1(a)–(d), the total strain rate or increment $\dot{\varepsilon}$ can be decomposed into elastic and inelastic portions $\dot{\varepsilon}^e$ and $\dot{\varepsilon}^i$, where the inelastic portion is composed of plastic and damage terms $\dot{\varepsilon}^p$ and $\dot{\varepsilon}^d$, thus

$$\dot{\varepsilon} = \dot{\varepsilon}^e + \dot{\varepsilon}^i = \dot{\varepsilon}^e + \dot{\varepsilon}^p + \dot{\varepsilon}^d. \tag{1}$$

Denoting by $\mathbf{C}^e$ and $\mathbf{D}^e = (\mathbf{C}^e)^{-1}$ the elastic compliance and stiffness matrices, we have

$$\dot{\varepsilon}^e = \mathbf{C}^e \dot{\sigma} \tag{2}$$

and

$$\dot{\sigma} = \mathbf{D}^e \dot{\varepsilon}^e = \mathbf{D}^e(\dot{\varepsilon} - \dot{\varepsilon}^i) = \dot{\sigma}^e + \dot{\sigma}^i = \dot{\sigma}^e + \dot{\sigma}^p + \dot{\sigma}^d \tag{3}$$

where

$$\dot{\sigma}^e = \mathbf{D}^e \dot{\varepsilon}, \quad \dot{\sigma}^p = -\mathbf{D}^e \dot{\varepsilon}^p, \quad \dot{\sigma}^d = -\mathbf{D}^e \dot{\varepsilon}^d, \quad \dot{\sigma}^i = -\mathbf{D}^e \dot{\varepsilon}^i. \tag{4}$$

Figures 1(b)–(d) present the decomposition of the total stress rate associated with the specified strain rate into elastic and inelastic components. It is seen that $\dot{\sigma}^i$ now plays the

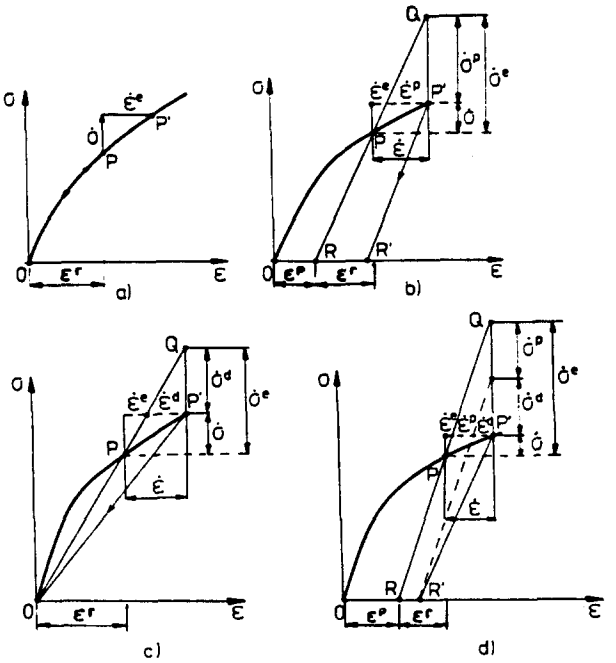

Fig. 1. Total stress and strain rate components: (a) elastic; (b) elastic–plastic; (c) elastic–damage; (d) elastic–plastic–damage.

role of a relaxation stress rate imposed upon the elastic stress rate $\dot{\sigma}^e$ associated with the specified strain rate.† The incremental (or rate) constitutive equations will have the form

$$\dot{\varepsilon} = \mathbf{C}\dot{\sigma}, \quad \dot{\sigma} = \mathbf{D}\dot{\varepsilon}, \quad \mathbf{C} = \mathbf{D} \tag{5}$$

where C and D are the tangent compliance and stiffness modulus matrices. It is assumed that these matrices depend on stress or strain states and on a set of hardening and damage state variables κ and ω, thus

$$\mathbf{C} = \mathbf{C}(\sigma, \varepsilon, \kappa, \omega), \quad \mathbf{D} = \mathbf{D}(\sigma, \varepsilon, \kappa, \omega). \tag{6}$$

The state variables will be defined later. Their evolution rules will be more precisely formulated by introducing the concepts of *yield* and *damage surfaces* specified by

$$F(\sigma, \kappa) = 0 \quad \text{or} \quad \phi(\varepsilon, \kappa) = 0 \tag{7}$$

and

$$D(\sigma, \omega) = 0 \quad \text{or} \quad \Delta(\varepsilon, \omega) = 0 \tag{8}$$

where $F = 0$, $D = 0$ are the yield and damage surfaces specified in stress space, whereas $\phi = 0$ and $\Delta = 0$ are the respective surfaces in strain space. Thus, for states represented by points lying within the domain enclosed by the yield surface in the stress or strain spaces, there is no plastic deformation process taking place whereas plastic flow occurs whenever $F = \dot{F} = 0$. Similarly, the damage process occurs when $D = \dot{D} = 0$. At the intersection of the damage and yield surfaces a "corner" regime occurs and the incremental rules are properly modified.

Using decompositions (1) and (3), we can write

† The matrix notation is used in eqns (2)–(4) and subsequent formulas. Thus $\mathbf{Aa} = A_{ij}b_j$, $\mathbf{Cd} = C_{ijkl}d_{kl}$ denotes the product of matrices of different orders. The scalar product is denoted by $\mathbf{a}\cdot\mathbf{b} = \mathbf{a}^T\mathbf{b} = a_ib_i$ and the tensor product by $\mathbf{a}\otimes\mathbf{b} = a_ib_j$.

$$\mathbf{C} = \mathbf{C}^e + \mathbf{C}^p + \mathbf{C}^d, \quad \mathbf{D} = \mathbf{D}^e + \mathbf{D}^p + \mathbf{D}^d \tag{9}$$

so that

$$\dot{\varepsilon}^e = \mathbf{C}^e\dot{\sigma}, \quad \dot{\varepsilon}^p = \mathbf{C}^p\dot{\sigma}, \quad \dot{\varepsilon}^d = \mathbf{C}^d\dot{\sigma} \tag{10}$$

$$\dot{\sigma}^e = \mathbf{D}^e\dot{\varepsilon}, \quad \dot{\sigma}^p = \mathbf{D}^p\dot{\varepsilon}, \quad \dot{\sigma}^d = \mathbf{D}^d\dot{\varepsilon}. \tag{11}$$

Thus, in the elastic region there is $\mathbf{D}^d = \mathbf{D}^p = \mathbf{C}^p = \mathbf{C}^d = \mathbf{0}$. When only damage takes place then $\mathbf{C}^p = \mathbf{D}^p = \mathbf{0}$; when only plastic flow occurs, then $\mathbf{C}^d = \mathbf{D}^d = \mathbf{0}$, whereas for the case when coupled damage–plastic flow processes occur all matrices of eqns (9) participate in the constitutive relation.

Assume now that the total strain consists of the sum of reversible and irreversible (plastic) strains, as shown in Fig. 1, thus

$$\varepsilon = \varepsilon^r + \varepsilon^p = \mathbf{C}^e\sigma + \varepsilon^p. \tag{12}$$

In fact, the damage strain is reversible and during unloading, no permanent strain develops due to the damage process. In eqn (12), the matrix $\mathbf{C}^e$ represents the secant compliance moduli tensor, and it is the same as the tensor of tangent moduli in the case of linear elasticity. Differentiating eqn (12), we obtain

$$\dot{\varepsilon} = \mathbf{C}^e\dot{\sigma} + \dot{\mathbf{C}}^e\sigma + \dot{\varepsilon}^p = \dot{\varepsilon}^e + \dot{\varepsilon}^d + \dot{\varepsilon}^p. \tag{13}$$

In view of eqns (10) and (13) it follows, with the assumption of linear elasticity, that

$$\mathbf{C}^d\dot{\sigma} = \dot{\mathbf{C}}^e\sigma \tag{14}$$

and similar relations are derived for the stiffness moduli. Inverting eqn (12), we have

$$\sigma = \mathbf{D}^e(\varepsilon - \varepsilon^p) \quad \text{and} \quad \dot{\sigma} = \mathbf{D}^e\dot{\varepsilon} - \mathbf{D}^e\dot{\varepsilon}^p + \dot{\mathbf{D}}^e(\varepsilon - \varepsilon^p) \tag{15}$$

and in view of eqns (11) and (15), there is

$$\mathbf{D}^d\dot{\varepsilon} = \dot{\mathbf{D}}^e(\varepsilon - \varepsilon^p) \tag{16}$$

where $\mathbf{D}^e$ denotes the secant stiffness moduli matrix. Relations (14) and (16) impose constraints on matrices $\mathbf{C}^d$ and $\mathbf{D}^d$.

Now, let us discuss consecutively plasticity, damage or degradation and coupled effects in concrete.

2.1. *Plasticity*

Assume, as usual, that the yield surface depends on both stress and a state variable κ, thus

$$F(\sigma, \kappa) = 0 \tag{17}$$

where the evolution rule for κ takes a general form

$$\kappa = \kappa(\varepsilon^p). \tag{18}$$

It should be noted that the flow rule is not necessarily associated with the yield surface

$$\dot{\boldsymbol{\varepsilon}}^{\mathrm{p}} = \dot{\lambda}\mathbf{m}, \quad \dot{\lambda} \geqslant 0 \tag{19}$$

where $\mathbf{m}$ specifies the direction of plastic flow. The scalar multiplier $\dot{\lambda}$ is determined from the consistency condition

$$\dot{\mathbf{F}} = \mathbf{F}_{,\sigma} \cdot \dot{\boldsymbol{\sigma}} + \mathbf{F}_{,\kappa} \cdot \dot{\kappa} = 0 \tag{20}$$

which provides

$$\dot{\lambda} = \frac{1}{H}\mathbf{f} \cdot \dot{\boldsymbol{\sigma}} \tag{21}$$

so that

$$\dot{\boldsymbol{\varepsilon}}^{\mathrm{p}} = \frac{1}{H}(\mathbf{m} \otimes \mathbf{f})\dot{\boldsymbol{\sigma}} = \mathbf{C}^{\mathrm{p}}\dot{\boldsymbol{\sigma}} \tag{22}$$

where

$$\mathbf{f} = \frac{\mathbf{F}_{,\sigma}}{|\mathbf{F}_{,\sigma}|}; \quad |\mathbf{F}_{,\sigma}| = (\mathbf{F}_{,\sigma} \cdot \mathbf{F}_{,\sigma})^{1/2} \tag{23}$$

and the comma preceding an index denotes partial differentiation. For hardening behaviour the loading–unloading conditions can be specified in terms of the stress rate, so that

$$\mathbf{C}^{\mathrm{p}} = 0 \quad \text{when} \quad \mathbf{f} \cdot \dot{\boldsymbol{\sigma}} \leqslant 0 \quad \text{and} \quad F = 0 \quad \text{or} \quad F < 0. \tag{24}$$

However, for softening behaviour, we have to specify loading–unloading conditions in terms of the strain rate.

2.2. *Degradation*

The specific elastic stress energy per unit volume U is now a function of both stress and the damage variable ω, $U = U(\boldsymbol{\sigma}, \omega)$ so that

$$\boldsymbol{\varepsilon}^{\mathrm{r}}(\boldsymbol{\sigma}, \omega) = \frac{\partial U(\boldsymbol{\sigma}, \omega)}{\partial \boldsymbol{\sigma}}. \tag{25}$$

The strain rate is obtained from eqn (25)

$$\dot{\boldsymbol{\varepsilon}}^{\mathrm{r}} = \frac{\partial^2 U}{\partial \boldsymbol{\sigma} \otimes \partial \boldsymbol{\sigma}}\dot{\boldsymbol{\sigma}} + \frac{\partial^2 U}{\partial \boldsymbol{\sigma} \otimes \partial \omega}\dot{\omega} = \dot{\boldsymbol{\varepsilon}}^{\mathrm{e}} + \dot{\boldsymbol{\varepsilon}}^{\mathrm{d}}. \tag{26}$$

Assume that the damaged surface is specified in terms of stress and the damage variable ω, thus

$$D(\boldsymbol{\sigma}, \omega) = 0. \tag{27}$$

Alternatively, one can specify the damage surface in terms of strain, so that

$$\Delta(\boldsymbol{\varepsilon}, \omega) = D[\mathbf{D}^{\mathrm{e}}(\boldsymbol{\varepsilon} - \boldsymbol{\varepsilon}^{\mathrm{p}}), \omega] = 0. \tag{28}$$

Some authors, notably Dougill (1976), Krajcinovic and Fonseka (1981), Bazant and Kim (1979) assume normality between the stress rate $\dot{\boldsymbol{\sigma}}^{\mathrm{d}}$ and the damage surface formulated in strain space, so that

$$\dot{\sigma}^{d} = \dot{\Lambda}\frac{\partial \Delta}{\partial \varepsilon}. \tag{29}$$

This rule is equivalent to the assumption of normality of the damage strain rate $\dot{\varepsilon}^{d}$ to the damage surface formulated in stress space, namely

$$\dot{\varepsilon}^{d} = \dot{\lambda}\frac{\partial D}{\partial \sigma}. \tag{30}$$

In fact since $D = \Delta = 0$ it can be written, in view of eqn (28), that

$$\frac{\partial \Delta}{\partial \varepsilon} = \frac{\partial D}{\partial \sigma}\frac{\partial \sigma}{\partial \varepsilon} = \frac{\partial D}{\partial \sigma}\mathbf{D}^{e}. \tag{31}$$

Multiplying both sides of eqn (31) by $\mathbf{C}^{e} = (\mathbf{D}^{e})^{-1}$, the equivalence of eqns (29) and (30) is demonstrated.

It should be noted that the implications of the associated damage rule (29) or (30) are too restrictive, if we assume an isotropic material response. Consider, for instance, the case of pure shear for which $\sigma_{kk} = 0$. Starting from Hooke's law $\varepsilon_{kk} = 1/(3K)\sigma_{kk}$, the volumetric damage strain is specified as

$$\dot{\varepsilon}_{v}^{d} = \tfrac{1}{3}\sigma_{kk}\left(\frac{\dot{1}}{K}\right) = 0 \tag{32}$$

whereas the associated damage rule (30) would provide

$$\dot{\varepsilon}_{v}^{d} = \dot{\lambda}\frac{\partial D}{\partial \sigma_{kk}}. \tag{33}$$

To satisfy eqn (29), that is consistency between eqns (32) and (33), the gradient tensor to the damage surface should have no spherical component for $\sigma_{kk} = 0$. Only surfaces representing conditions such as Huber–Mises or Tresca, not depending on hydrostatic pressure satisfy this requirement. Such surfaces, however, cannot be used to represent the damage condition for concrete which should be pressure dependent. We can, of course, depart from the assumption of isotropy, by introducing the concept of a more general anisotropic structure of a damaged body. Whenever, for the sake of simplicity let the isotropy assumption be preserved, as a consequence the non-associated damage rules should be used in order to satisfy eqn (29) or eqn (30). The assumption of isotropic elastic degradation is, of course, controversial, but it is our assessment that there are two reasons for it to be justified. The first is a lack of experimental data sufficient to identify material parameters for more complex models, and the second involves the review of experimental evidence related to the initial stages of degradation where both microcrack locations and directions of propagation are random. Therefore, in the pre-critical range a serious departure from this assumption can be observed only for stress-states close to ultimate strength. In the post-critical range the present model is intended to be supplemented by a localization model at the element level. Such effects as directionality of crack propagation and closure of cracks, when the load direction is reversed, will be considered in the future as ingredients in the localization model.

Another possible description of the elastic degradation is based on the thermodynamical considerations and can be found in the papers by Lemaitre (1985) and by Simo *et al.* (1987).

Instead of formulating directly the damage rule, we can use the energy balance equation for a representative element and specify the rate of dissipation associated with damage. Considering a quasistatic damage process and neglecting thermal effects, we can write

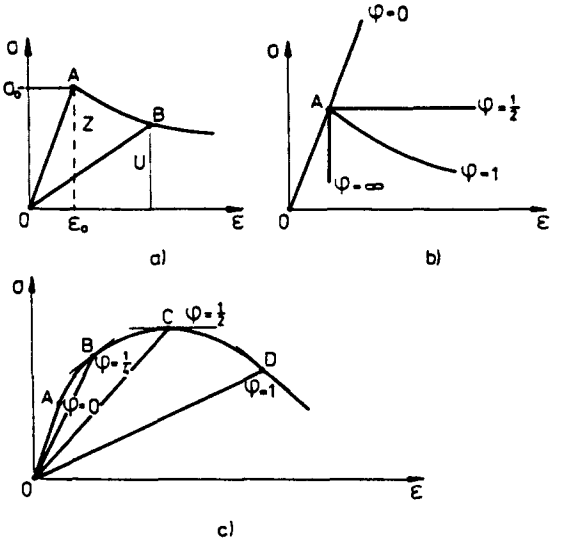

Fig. 2. Damage proportionality factor: (a) $\phi = 1$; (b) model behaviour for different ϕ values; (c) continuous degradation process.

$$\dot{W} = \dot{U} + \dot{R} + \dot{Z} \tag{34}$$

where $\dot{W}$ is the rate of work of external tractions, $\dot{U}$ denotes the rate of elastic energy, $\dot{R}$ is the plastic dissipation rate and $\dot{Z}$ denotes the damage dissipation rate. For macroscopically homogeneous stress and strain states, the terms occurring in eqn (34) can be referred to the unit volume of the element. Let us note that in Griffith's theory the damage dissipation rate is expressed in terms of the specific surface energy and the rate of growth of crack area. In our approach, we do not explicitly specify the damage in terms of crack area. It will be assumed that $\dot{Z}$ constitutes a portion of the available work rate for fracture, that is

$$\dot{Z} = \phi(\dot{W} - \dot{R}) \tag{35}$$

where ϕ is a proportionality factor. If there is no plastic flow, then $\dot{R} = 0$, and eqn (35) specifies the portion of external work rate dissipated in damage. In the uniaxial case, eqn (35) then provides a relation between tangent and secant moduli of the stress–strain curve. In fact, since $\dot{W} = \sigma\dot{\varepsilon}$, $\dot{U} = 1/2\sigma\dot{\varepsilon} + 1/2\dot{\sigma}\varepsilon$, $\dot{R} = 0$, from eqn (35) it follows that

$$\frac{\varepsilon}{\sigma}\frac{\mathrm{d}\sigma}{\mathrm{d}\varepsilon} = \frac{E_t}{E_s} = 1 - 2\phi \tag{36}$$

where $E_t = \mathrm{d}\sigma/\mathrm{d}\varepsilon$ denotes the tangent modulus and $E_s = \sigma/\varepsilon$ is the secant modulus. Figure 2 illustrates the character of stress–strain curves for different values of ϕ. When $\phi = 1/2$, then $\dot{Z} = \dot{U} = 1/2\dot{W}$, $E_t = 0$ and the stress–strain curve resembles that of perfectly plastic behaviour. When $\phi = 1$, there is $\dot{U} = 0$, $\dot{Z} = \dot{W}$ and $\sigma\varepsilon = \text{const}$. Perfectly brittle behaviour corresponds to $\phi \to \infty$. For $\phi > 1/2$, a stable stress–strain curve is generated. In writing eqn (35), we exclude the possibility of an uncontrolled progressing damage at fixed strain of the representative element. Such progression may only occur for an inhomogeneous system containing a damage zone and a surrounding elastic material domain.

For a more general formulation, the scalar factor ϕ need not be constant but can change during the deformation process. Note that for an arbitrary stress–strain curve, the scalar function ϕ can be identified from eqn (36) by knowing secant and tangent moduli. It can be assumed that for a sufficiently general class of stress–strain curves the factor ϕ increases along the curve. It can therefore be assumed to be an independent damage variable specified in terms of the compliance moduli. It turns out that by using eqn (35) we can derive the constitutive equations for the damage process and next couple it with the plastic deformation process.

2.3. *Constitutive relations for the axisymmetric case*

Let us first formulate the constitutive relations in terms of unordered principal stresses for a case when two principal stresses are equal, $\sigma_2 = \sigma_3$. Such a state is typical in testing of cylindrical specimens subjected to axial extension or compression and lateral confinement pressure (triaxial tests). Introduce the following stress vector:

$$\tilde{\sigma} = \begin{bmatrix} p \\ q \end{bmatrix} \tag{37}$$

where

$$p = -\tfrac{1}{3}(\sigma_1 + 2\sigma_2), \quad q = \sigma_2 - \sigma_1 \tag{38}$$

are the hydrostatic and shear stresses. The conjugate strain vector is

$$\tilde{\varepsilon} = \begin{bmatrix} \varepsilon_v \\ \varepsilon_q \end{bmatrix} \tag{39}$$

where

$$\varepsilon_v = -(\varepsilon_1 + 2\varepsilon_2), \quad \varepsilon_q = \tfrac{2}{3}(\varepsilon_2 - \varepsilon_1) \tag{40}$$

so that

$$\tilde{\sigma} \cdot \tilde{\varepsilon} = p\varepsilon_v + q\varepsilon_q = \sigma_1\varepsilon_1 + 2\sigma_2\varepsilon_2. \tag{41}$$

Hooke's law for specified stress and strain states has the form

$$\tilde{\varepsilon} = \tilde{\mathbf{C}}^e\tilde{\sigma}, \quad \tilde{\mathbf{C}}^e = \begin{bmatrix} \dfrac{1}{K} & 0 \\ 0 & \dfrac{1}{3G} \end{bmatrix} = \begin{bmatrix} T & 0 \\ 0 & S \end{bmatrix} \tag{42}$$

where K and G are the bulk and shear moduli. The compliance moduli are denoted as

$$T = \frac{1}{K}, \quad S = \frac{1}{3G} \tag{43}$$

and the specific elastic stress energy for an isotropic material takes the form

$$U = \tfrac{1}{2}(Tp^2 + Sq^2). \tag{44}$$

It will be assumed that the compliance moduli constitute the damage vector, so that

$$\tilde{\omega} = \begin{bmatrix} T \\ S \end{bmatrix}. \tag{45}$$

In fact, due to progressive cracking both T and S will vary, so they can be assumed to represent the damage state of the element. This approach reduces the number of variables and can be related to hypoelastic models with variable elastic moduli.

Differentiating eqn (44) one obtains

$$\dot{U} = \tfrac{1}{2}p^2\dot{T} + \tfrac{1}{2}q^2\dot{S} + Tp\dot{p} + Sq\dot{q} \tag{46}$$

and

$$\dot{W} - \dot{R} = \bar{\sigma}(\dot{\bar{\varepsilon}} - \dot{\bar{\varepsilon}}^{\mathrm{p}}) = \bar{\sigma}(\bar{\mathbf{C}}^{\mathrm{e}}\dot{\bar{\sigma}} + \dot{\bar{\mathbf{C}}}^{\mathrm{e}}\bar{\sigma}) = p^2\dot{T} + q^2\dot{S} + Tp\dot{p} + Sq\dot{q}. \tag{47}$$

From energy balance (34), it follows that

$$\dot{Z} = \dot{W} - \dot{R} - \dot{U} = \tfrac{1}{2}p^2\dot{T} + \tfrac{1}{2}q^2\dot{S} \tag{48}$$

and condition (35) provides the equality

$$(\tfrac{1}{2} - \phi)(p^2\dot{T} + q^2\dot{S}) = \phi(Tp\dot{p} + Sq\dot{q}). \tag{49}$$

The consistency condition for the damage surface

$$D(\bar{\sigma} + \dot{\bar{\sigma}}, \bar{\omega} + \dot{\bar{\omega}}) = 0 \tag{50}$$

furnishes the second equation specifying the evolution rule for T and S, namely

$$D_{,T}\dot{T} + D_{,S}\dot{S} = -(D_{,p}\dot{p} + D_{,q}\dot{q}). \tag{51}$$

A solution of eqns (49) and (51) takes the following form:

$$\dot{\bar{\omega}} = \bar{\mathbf{\Omega}}\dot{\bar{\sigma}} \tag{52}$$

where

$$\bar{\mathbf{\Omega}} = \frac{1}{\Delta}\begin{bmatrix} \phi TpD_{,S} + (\tfrac{1}{2} - \phi)q^2D_{,p} & \phi SqD_{,S} + (\tfrac{1}{2} - \phi)q^2D_{,q} \\ -\phi TpD_{,T} + (\tfrac{1}{2} - \phi)p^2D_{,p} & -\phi SqD_{,T} + (\tfrac{1}{2} - \phi)p^2D_{,q} \end{bmatrix} \tag{53}$$

and

$$\Delta = (\tfrac{1}{2} - \phi)(p^2D_{,S} - q^2D_{,T}). \tag{54}$$

Equation (52) can be regarded as the evolution rule for the damage vector $\bar{\omega}$ relating its rate to the stress rate during the active damage process. In view of eqn (41) the damage strain rate can now be presented as

$$\dot{\bar{\varepsilon}}^{\mathrm{d}} = \bar{\mathbf{C}}^{\mathrm{d}}\dot{\bar{\sigma}} = \dot{\bar{\mathbf{C}}}^{\mathrm{e}}\bar{\sigma} = \bar{\mathbf{A}}\dot{\bar{\omega}} = \bar{\mathbf{A}}\bar{\mathbf{\Omega}}\dot{\bar{\sigma}} \tag{55}$$

hence

$$\bar{\mathbf{C}}^{\mathrm{d}} = \bar{\mathbf{A}}\bar{\mathbf{\Omega}} \tag{56}$$

where

$$\bar{\mathbf{A}} = \begin{bmatrix} p & 0 \\ 0 & q \end{bmatrix}. \tag{57}$$

To obtain eqn (55) we used the identity

$$\dot{\mathbf{C}}^{c}\dot{\boldsymbol{\sigma}} = \begin{bmatrix} \dot{T} & 0 \\ 0 & \dot{S} \end{bmatrix}\begin{bmatrix} p \\ q \end{bmatrix} = \begin{bmatrix} p & 0 \\ 0 & q \end{bmatrix}\begin{bmatrix} \dot{T} \\ \dot{S} \end{bmatrix} = \bar{\mathbf{A}}\dot{\bar{\omega}}. \tag{58}$$

For $\Delta = 0$, relation (52) specifies the limit state corresponding to maximum stress. To avoid multiple limit points, a special form of the damage surface is assumed, namely

$$D = D(\bar{\sigma}, \phi) = 0 \tag{59}$$

and

$$\phi = \phi(T, S) = \phi(\bar{\omega}). \tag{60}$$

This means that the damage condition depends explicitly on the scalar function ϕ, which in turn depends on the compliance moduli T and S constituting the damage variable. The change of damage surface is therefore associated with the variation of ϕ. However, as the damage process can proceed at constant ϕ (cf. Fig. 2), T and S may vary for some loading paths lying inside the surface $D = 0$. Writing

$$D_{,S} = D_{,\phi}\phi_{,S}, \quad D_{,T} = D_{,\phi}\phi_{,T} \tag{61}$$

the expression for Δ takes the form

$$\Delta = (\tfrac{1}{2} - \phi)D_{,\phi}(p^2\phi_{,S} - q^2\phi_{,T}). \tag{62}$$

Assume now that $D_{,\phi} = 0$ only for $\phi = 1/2$. The damage surface then becomes the limit surface. For other values of ϕ, the function Δ should not vanish. This can be achieved by assuming that $\phi_{,T}$ and $\phi_{,S}$ have opposite signs.

The condition $\dot{Z} \geqslant 0$ occurring for an active damage process can be geometrically interpreted by calculating rates $\dot{T}$ and $\dot{S}$ from eqn (52) and substituting into eqn (48). We obtain

$$\dot{Z} = \mathbf{d}_1 \cdot \dot{\boldsymbol{\sigma}} \geqslant 0 \tag{63}$$

where

$$\mathbf{d}_1 = \frac{\phi}{1-2\phi}\begin{bmatrix} Tp \\ Sq \end{bmatrix} = \frac{\phi}{1-2\phi}\begin{bmatrix} \dfrac{\partial U}{\partial p} \\ \dfrac{\partial U}{\partial q} \end{bmatrix} \tag{64}$$

is the vector normal to the surface of constant stress energy $U = \text{const}$. On the other hand, the loading condition associated with the damage surface is expressed as

$$\mathbf{d}_2 \cdot \dot{\boldsymbol{\sigma}} \geqslant 0$$

where

$$\mathbf{d}_2 = \frac{1}{D_{,\phi}}\begin{bmatrix} D_{,p} \\ D_{,q} \end{bmatrix} \tag{65}$$

is the vector normal to the damage surface $D = 0$. Let us note that the matrix $\bar{\boldsymbol{\Omega}}$ specified by eqn (53) can be decomposed into two portions, namely

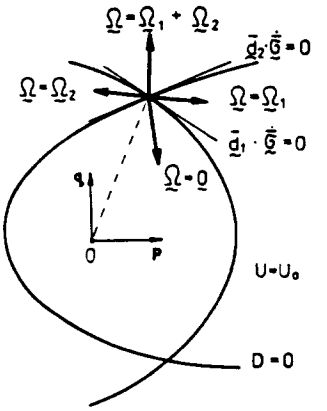

Fig. 3. Corner regime of damage model.

$$\bar{\Omega} = \bar{\Omega}_1 + \bar{\Omega}_2 \tag{66}$$

where

$$\bar{\Omega}_1 = \frac{1}{\Delta}\phi\begin{bmatrix} TpD_{,S} & SqD_{,S} \\ -TpD_{,T} & -S_qD_{,T} \end{bmatrix} = \frac{\phi}{(\frac{1}{2}-\phi)(p^2\phi_{,S}-q^2\phi_{,T})}\begin{bmatrix} \phi_{,S} \\ -\phi_{,T} \end{bmatrix}[Tp \quad Sq]$$

$$\bar{\Omega}_2 = \frac{1}{\Delta}(\tfrac{1}{2}-\phi)\begin{bmatrix} q^2D_{,p} & q^2D_{,q} \\ -p^2D_{,p} & -p^2D_{,q} \end{bmatrix} = \frac{1}{D_{,\phi}(p^2\phi_{,S}-q^2\phi_{,T})}\begin{bmatrix} q^2 \\ -p^2 \end{bmatrix}[D_{,p} \quad D_{,q}]. \tag{67}$$

Thus, when $\phi < 1/2$, the following unloading conditions are valid:

$$\begin{aligned} &\bar{\Omega}_1 = 0 \quad \text{when} \quad U < U_0 \quad \text{or} \quad U = U_0, \quad \bar{\mathbf{d}}_1 \cdot \dot{\bar{\sigma}} \leqslant 0 \\ &\bar{\Omega}_2 = 0 \quad \text{when} \quad D < 0 \quad \text{or} \quad D = 0, \quad \bar{\mathbf{d}}_2 \cdot \dot{\bar{\sigma}} \leqslant 0. \end{aligned} \tag{68}$$

For $\phi > 1/2$ the process is not controllable by the stress rate and the strain rate should be used. Here U_0 denotes the actual value of the stress energy reached during the previous loading history. Conditions (68) are typical "corner" unloading conditions governed by two surfaces $U = U_0$ and $D = 0$ (Fig. 3). Note that continuity conditions are satisfied for $\bar{\mathbf{d}}_1 \cdot \dot{\bar{\sigma}} = 0$ and $\bar{\mathbf{d}}_2 \cdot \dot{\bar{\sigma}} = 0$. It is seen that when $\bar{\Omega} = \bar{\Omega}_1$, the elastic moduli vary at constant ϕ. On the other hand, when $\bar{\Omega} = \bar{\Omega}_2$, the scalar function ϕ varies at vanishing damage dissipation rate, $\dot{Z} = 0$. When $\Omega = \Omega_1 + \Omega_2$, both variations of ϕ and of the elastic energy occurs.

Consider now the hardening rule associated with plastic deformation. Assume the following associated flow rule:

$$\dot{\bar{\varepsilon}}^p = \dot{\lambda}\bar{\mathbf{f}}, \quad \dot{\lambda} \geqslant 0 \tag{69}$$

where

$$\bar{\mathbf{f}} = \begin{bmatrix} f^p \\ f^q \end{bmatrix} = \frac{1}{|\mathbf{F}_{,\sigma}|}\begin{bmatrix} F_{,p} \\ F_{,q} \end{bmatrix}; \quad |\mathbf{F}_{,\sigma}| = (\mathbf{F}_{,\sigma} \cdot \mathbf{F}_{,\sigma})^{1/2} \tag{70}$$

is the normal unit vector to the yield surface $F = 0$. The following hardening variables are used to specify plastic hardening and coupling with damage:

$$\kappa = \begin{bmatrix} \kappa \\ \beta \end{bmatrix}. \tag{71}$$

The rates of κ and β are

$$\dot{\kappa} = |\dot{\varepsilon}_q^p|$$
$$\dot{\beta} = \dot{\varepsilon}_v^p + \alpha \dot{\varepsilon}_v^d. \tag{72}$$

provided both plastic deformation and damage develop simultaneously. Here κ corresponds to deviatoric hardening, whereas β represents the volumetric plastic hardening or softening and the damage effects which are accounted for only through the volumetric part of the damage strain. Parameter α is a weighting factor between plastic and damage volumetric strains. Denoting by C_p and C_q the respective terms of the matrix $\tilde{\mathbf{C}}^d$ specified by eqn (56) we may write

$$\dot{\varepsilon}_v^d = C_p \dot{p} + C_q \dot{q}. \tag{73}$$

From the consistency condition

$$\dot{F} = \mathbf{F}_{,\sigma} \cdot \dot{\sigma} + F_{,\kappa} \dot{\kappa} + F_{,\beta} \dot{\beta} \tag{74}$$

and the flow rule, we obtain

$$\dot{\tilde{\mathbf{C}}}^p = \frac{1}{H} \begin{bmatrix} F_{,p} \\ F_{,q} \end{bmatrix} [F_{,p} + F_{,\beta} \alpha C_p, \quad F_{,q} + F_{,\beta} \alpha C_q] \tag{75}$$

where

$$H = -(F_{,\kappa} |F_{,q}| + F_{,\beta} F_{,p}). \tag{76}$$

Thus despite the associated flow rule (69), the resulting relation

$$\dot{\varepsilon}^p = \tilde{\mathbf{C}}^p \dot{\sigma} \tag{77}$$

is generated by a non-symmetric compliance matrix $\tilde{\mathbf{C}}^p$. This nonsymmetry is due to the effect of coupling occurring between damage strain and plastic hardening. When both damage and plastic deformation occur simultaneously, the stress state is represented by a line created by the intersection of two surfaces. Since it is assumed that the plastic strain has no effect on the damage, but the damage strain effects plastic hardening, this results in nonsymmetry of $\tilde{\mathbf{C}}^p$. Only when $\dot{\varepsilon}^d = 0$ or $\alpha = 0$ the matrix $\tilde{\mathbf{C}}^p$ is symmetric. The loading condition for the plastic surface has the form

$$\tilde{\mathbf{r}} \cdot \dot{\sigma} \geqslant 0 \tag{78}$$

$$\tilde{\mathbf{r}} = \begin{bmatrix} F_{,p} + F_{,\beta} \alpha C_p \\ F_{,q} + F_{,\beta} \alpha C_q \end{bmatrix}. \tag{79}$$

2.4. *Constitutive model for multiaxial stress and strain states*

The previous formulation can now easily be extended to general stress and strain states. Introduce the stress invariants

$$J_1' = \sigma_{kk} = \sigma_1+\sigma_2+\sigma_3 = \sigma_x+\sigma_y+\sigma_z$$
$$J_2 = \tfrac{1}{2}s_{ij}s_{ij} = \tfrac{1}{2}(s_1^2+s_2^2+s_3^2) = \tfrac{1}{2}(s_x^2+s_y^2+s_z^2)+\tau_{xy}^2+\tau_{yz}^2+\tau_{zx}^2$$
$$J_3 = \tfrac{1}{3}s_{ij}s_{ki}s_{kj} = s_1s_2s_3 = \begin{vmatrix} s_x & \tau_{xy} & \tau_{zx} \\ \tau_{xy} & s_y & \tau_{yz} \\ \tau_{zx} & \tau_{yz} & s_z \end{vmatrix} \tag{80}$$

where $s_{ij} = \sigma_{ij} - 1/3\sigma_{kk}\delta_{ij}$ denotes the stress deviator. An alternative set of invariants

$$\sigma_0 = \tfrac{1}{3}J_1', \quad \rho = \frac{2}{\sqrt{3}}\sqrt{J_2}, \quad \theta = \tfrac{1}{3}\arccos\frac{4J_3}{\rho^3} \tag{81}$$

is more useful in formulating the constitutive relations. The principal stresses are now expressed as follows in terms of σ_0, ρ, and θ

$$\begin{bmatrix}\sigma_1\\ \sigma_2\\ \sigma_3\end{bmatrix} = \begin{bmatrix}\sigma_0\\ \sigma_0\\ \sigma_0\end{bmatrix} + \rho\begin{bmatrix}\cos\theta\\ \cos(\theta-2.3\pi)\\ \cos(\theta+2/3\pi)\end{bmatrix}. \tag{82}$$

Let us assume that p and q used in the axisymmetric case can be related to invariants (81), in the form

$$p = -\sigma_0$$
$$q = \tfrac{3}{2}g(\theta)\rho \tag{83}$$

where $g(\theta)$ accounts for the dependence on J_3. When $\phi_2 = \sigma_3$ and $\theta = \pi/3$ and p and q specified by eqns (83) become the stress components related to the triaxial test as seen in eqns (38), it is assumed that $g(\pi/3) = 1$. By using eqns (83) we assume that the yield or damage condition is expressed in the special form $F(\sigma_0, g(\theta)\rho) = 0$. This means, in particular, that the shape on the deviatoric plane is independent on the hydrostatic pressure. The stress rate $\dot{\sigma}$ in an axisymmetric case can now be related to principal stress rates or to stress rates in the reference system x, y, z. Thus

$$\dot{\tilde{\sigma}} = \mathbf{Q}_{(2\times 3)}\dot{\sigma}_{(3)} \quad \text{or} \quad \dot{\tilde{\sigma}} = \mathbf{Q}_{(2\times 6)}\dot{\sigma}_{(6)} \tag{84}$$

where

$$\sigma_{(3)} = [\sigma_1, \ \sigma_2, \ \sigma_3]^T$$
$$\sigma_{(6)} = [\sigma_x, \ \sigma_y, \ \sigma_z, \ \tau_{xy}, \ \tau_{yz}, \ \tau_{zx}]^T \tag{85}$$

and

$$\mathbf{Q}_{(2\times 3)} = \begin{bmatrix} p_{,\sigma_1} & p_{,\sigma_2} & p_{,\sigma_3} \\ q_{,\sigma_1} & q_{,\sigma_2} & q_{,\sigma_3} \end{bmatrix}$$
$$\mathbf{Q}_{(2\times 6)} = \begin{bmatrix} p_{,\sigma_x} & p_{,\sigma_y} & p_{,\sigma_z} & p_{,\tau_{xy}} & p_{,\tau_{yz}} & p_{,\tau_{zx}} \\ q_{,\sigma_x} & q_{,\sigma_y} & q_{,\sigma_z} & q_{,\tau_{xy}} & q_{,\tau_{yz}} & q_{,\tau_{zx}} \end{bmatrix}. \tag{86}$$

The matrices of elastic compliance are expressed in terms of T and S in a form

$$\mathbf{C}^{e}_{(3\times 3)} = \begin{bmatrix} \frac{T}{9}+S & \frac{T}{9}-\frac{S}{2} & \frac{T}{9}-\frac{S}{2} \\ \frac{T}{9}-\frac{S}{2} & \frac{T}{9}+S & \frac{T}{9}-\frac{S}{2} \\ \frac{T}{9}-\frac{S}{2} & \frac{T}{9}-\frac{S}{2} & \frac{T}{9}+S \end{bmatrix} \tag{87}$$

and in an abbreviated form

$$\mathbf{C}^{e}_{(6\times 6)} = \begin{bmatrix} \mathbf{C}^{e}_{(3\times 3)} & \mathbf{0}_{(3\times 3)} \\ \mathbf{0}_{(3\times 3)} & 3S\mathbf{I}_{(3\times 3)} \end{bmatrix} \tag{88}$$

where **0** denotes the null matrix and **I** the unit matrix. The following equalities can be expressed as:

$$\begin{aligned} \dot{\mathbf{C}}^{e}_{(3\times 3)}\boldsymbol{\sigma}_{(3)} &= \mathbf{A}_{(3\times 2)}\dot{\boldsymbol{\omega}} \\ \dot{\mathbf{C}}^{e}_{(6\times 6)}\boldsymbol{\sigma}_{(6)} &= \mathbf{A}_{(6\times 2)}\dot{\boldsymbol{\omega}} \end{aligned} \tag{89}$$

where

$$\mathbf{A}_{(3\times 2)} = \begin{bmatrix} -\frac{p}{3} & \sigma_1-\frac{1}{2}(\sigma_2+\sigma_3) \\ -\frac{p}{3} & \sigma_2-\frac{1}{2}(\sigma_1+\sigma_3) \\ -\frac{p}{3} & \sigma_3-\frac{1}{2}(\sigma_1+\sigma_2) \end{bmatrix} \tag{90}$$

and

$$\mathbf{A}_{(6\times 2)} = \begin{bmatrix} -\frac{p}{3} & \sigma_x-\frac{1}{2}(\sigma_y+\sigma_z) \\ -\frac{p}{3} & \sigma_y-\frac{1}{2}(\sigma_x+\sigma_z) \\ -\frac{p}{3} & \sigma_z-\frac{1}{2}(\sigma_x+\sigma_y) \\ 0 & 3\tau_{xy} \\ 0 & 3\tau_{yz} \\ 0 & 3\tau_{zx} \end{bmatrix} \tag{91}$$

The damage strain rates now are

$$\begin{aligned} \dot{\boldsymbol{\varepsilon}}^{d}_{(3)} &= \mathbf{C}^{d}_{(3\times 3)}\dot{\boldsymbol{\sigma}}_{(3)} \\ \dot{\boldsymbol{\varepsilon}}^{d}_{(6)} &= \mathbf{C}^{d}_{(6\times 6)}\dot{\boldsymbol{\sigma}}_{(6)} \end{aligned} \tag{92}$$

where the matrices $\mathbf{C}^{d}_{(3\times 3)}$ and $\mathbf{C}^{d}_{(6\times 6)}$ are specified as

$$\begin{aligned} \mathbf{C}^{d}_{(3\times 3)} &= \mathbf{A}_{(3\times 2)}\bar{\boldsymbol{\Omega}}\mathbf{Q}_{(2\times 3)} \\ \mathbf{C}^{d}_{(6\times 6)} &= \mathbf{A}_{(6\times 2)}\bar{\boldsymbol{\Omega}}\mathbf{Q}_{(2\times 6)}. \end{aligned} \tag{93}$$

The stress gradient of the yield condition $F(\sigma, \kappa) = 0$ can be calculated by using gradient expressions $\mathbf{F}_{,\sigma}$, namely

$$\mathbf{F}_{,\sigma} = \mathbf{F}_{,\sigma}\mathbf{Q}. \tag{94}$$

The flow rule is therefore presented as

$$\begin{aligned} \dot{\boldsymbol{\varepsilon}}^{\mathrm{p}}_{(3\times 3)} &= \mathbf{C}^{\mathrm{p}}_{(3\times 3)}\dot{\boldsymbol{\sigma}}_{(3)} \\ \dot{\boldsymbol{\varepsilon}}^{\mathrm{p}}_{(6\times 6)} &= \mathbf{C}^{\mathrm{p}}_{(6\times 6)}\dot{\boldsymbol{\sigma}}_{(6)} \end{aligned} \tag{95}$$

where

$$\begin{aligned} \mathbf{C}^{\mathrm{p}}_{(3\times 3)} &= \mathbf{Q}^{\mathrm{T}}_{(2\times 3)}\bar{\mathbf{C}}^{\mathrm{p}}\mathbf{Q}_{(2\times 3)} \\ \mathbf{C}^{\mathrm{p}}_{(6\times 6)} &= \mathbf{Q}^{\mathrm{T}}_{(2\times 6)}\bar{\mathbf{C}}^{\mathrm{p}}\mathbf{Q}_{(2\times 6)} \end{aligned} \tag{96}$$

and the vectors occurring in loading–unloading conditions are

$$\begin{aligned} \mathbf{f}_{(3)} &= \bar{\mathbf{f}}\mathbf{Q}_{(2\times 3)}, \quad \mathbf{d}_{(3)} = \bar{\mathbf{d}}\mathbf{Q}_{(2\times 3)} \\ \mathbf{f}_{(6)} &= \bar{\mathbf{f}}\mathbf{Q}_{(2\times 6)}, \quad \mathbf{d}_{(6)} = \bar{\mathbf{d}}\mathbf{Q}_{(2\times 6)}. \end{aligned} \tag{97}$$

2.5. *Constitutive model for variable loading*

So far, we have assumed a linear elastic unloading within the domain enclosed by the yield and damage surfaces. Since during unloading or reverse loading irreversible deformations occur, and hysteretic behaviour is observed for cyclic loading, we can resort to a description of unloading or reloading phenomena similar to that proposed for soils by Mróz and Norris (1982), and Mróz and Pietruszczak (1973), and applying a multisurface formulation. A model version called INS will be used and further modified in order to describe more realistically cyclic concrete response.

In that model an active surface is constructed during unloading, and it is similar to the yield surface reached during the loading process and affine to it at the point from which unloading started. The yield surface reached during the loading process will now be called the maximum loading surface and the point of unloading will be called the reversal point. The direction of the plastic flow is normal to the active surface. The value of the plastic strain increment depends on the size of the active surface in comparison with the yield surface and on a value of the plastic hardening modulus at a conjugate point. The conjugate point lies on the maximum loading surface where its gradient has the same direction as the gradient of the active surface at the actual stress point. The increment of plastic strain can be described as:

$$\dot{\boldsymbol{\varepsilon}}^{\mathrm{p}} = \frac{1}{h(H,\gamma)}(\mathbf{r}\cdot\dot{\boldsymbol{\sigma}})\mathbf{f} \tag{98}$$

where

$$\gamma = \frac{R_k}{R}$$

R_k, R are the dimensions of the active ($F_k = 0$) and maximum loading ($F = 0$) surfaces, $\mathbf{f}$ the unit vector normal to the maximum loading surface at the conjugate point, H the plastic hardening modulus at the conjugate point, h the plastic modulus at the actual point, and $\mathbf{r}$ the loading vector (cf. eqn (79)).

When the loading direction is subsequently changed, a new set of active surfaces is created. They are also tangential to the previous surface at the reversal point. This procedure ensures that the active surfaces cannot intersect, and when a point lies on two of them, they

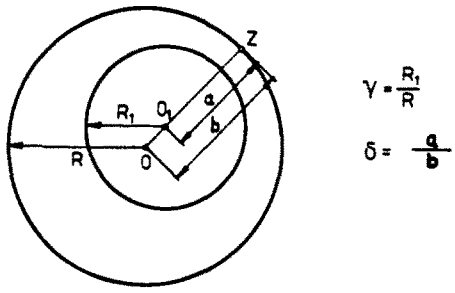

Fig. 4. Geometrical relations between active and maximum loading surfaces.

should coincide. There is only one exception—the reversal point. When it is reached a second time, the actual and previous surfaces can only be tangential. In this case an apparent discontinuity on the otherwise smooth stress–strain curve is observed, because of a jump change in the magnitude of the plastic modulus h. From this point of view the reversal points are singular.

This disadvantage can be eliminated by changing the evolution rule for the active surfaces. The active surface should not be tangential to the yield or previous surface at the reversal point. It must move into the domain enclosed by the maximum loading surface.

In the classical multisurface model the active surface is defined by the reversal point and the ratio of the characteristic dimensions γ. Now it is necessary to add one more variable and parameter. Inside the maximum loading and active surfaces a characteristic point must be defined, e.g. the centre. Let us assume that the centre of the active surface always lies on the line joining the maximum loading surface centre and the reversal point. The active surface centre divides this segment in a precise ratio

$$\delta = \frac{a}{b} \tag{99}$$

where a is the distance between the active surface centre and the reversal point and b is the distance between the centre of the maximum loading surface and the reversal point (Fig. 4). In the presented model the origin has been chosen as the characteristic point inside the yield surface.

Both parameters γ and δ can change from 0 to 1. Let us assume temporarily that the functional dependence between γ and δ can be established (such that $\delta \geqslant \gamma$ in order to avoid intersection of these two surfaces). Such a function should satisfy the conditions

$$\gamma(0) = 0, \quad \gamma(1) = 1. \tag{100}$$

If a linear function was defined, this model would give the same result as the INS model. If the other function was used, the interior of the maximum loading surface would be divided into two sets of points. The first would consist of the points which could be reached using this evolution rule in a smooth way and the second the points which can be reached only after a jump in both γ and δ. In this case the result would be the same as at the reversal point—a corner or discontinuity in the stress–strain curve. Because this is an unwanted feature, the relation between γ and δ cannot be defined in advance. The simplest evolution rule without these disadvantages can be proposed in the following way.

Let us assume that at each point two different evolution rules are possible and the one that is used depends on the direction of a given stress increment. The first version causes a drift of the active surface into the domain enclosed by the maximum loading surface, and it can be written in the form

$$\dot{\delta} = \begin{cases} \dfrac{\delta}{\gamma}\dot{\gamma} & \text{if } \gamma \neq 0\,(\delta < 1) \\ c_0\dot{\gamma} & \text{if } \gamma = 0\,(c_0 \geqslant 1) \end{cases} \tag{101}$$

where c_0 corresponds to the initial tangent of the $\delta(\gamma)$ curve. This evolution rule is used when the next stress state can be reached without any discontinuity and defines an envelope of the active surfaces inside the maximum loading surface. In the cases when the stress point moves outside the envelope, the second rule is applied. This rule does not result in drift but results only in the active surface expansion. It can be described by

$$\dot{\delta} = \frac{1-\delta}{1-\gamma}\dot{\gamma}. \tag{102}$$

This plastic model is a generalization of the multisurface model and can be reduced to the last version by the assumption $c_0 = 1$. It is also closely related to the subloading surface model by Hashiguchi (1980) or to the radial mapping version of the bounding surface model by Dafalias (1986). Instead of describing δ as ratio (99) it may be easier to introduce the position η of the centre of homothety between the active and maximum loading surfaces. The precise mathematical relation between old parameters γ and δ and a new variable η is given by

$$\gamma(1-\eta) = \delta - \eta. \tag{103}$$

When the projection centre of homothety coincides with the reversal point $\eta = 0$, and the value of η increases to 1, the projection centre moves toward the centre of the maximum loading surface. The first evolution rule describes such a process, whereas the second rule corresponds to the fixed position of the projection centre. Therefore, γ and η can be used as the model variables and the evolution rule can be specified in terms of the movement of the projection centre.

The plastic modulus function h has to satisfy the following conditions:

$$\begin{aligned} h(H,\gamma) &= \infty \quad \text{for } \gamma < \gamma^e \\ h(H,1) &= H \end{aligned} \tag{104}$$

where γ^e describes an elastic region and H the value of plastic modulus at the conjugate point.

The first condition means that inside the elastic region the plastic strain increment should equal zero. The second one assures the consistency with the classical plastic model. From the numerical point of view it is better to use the following function:

$$h(H,\gamma) = H + (M-H)\,(1-\gamma)^x \tag{105}$$

where the constant M should be much larger than the maximum value of H. This function satisfies the first condition only in the weakened form

$$h(H,\gamma) = M \quad \text{for} \quad \gamma < \gamma^e \tag{106}$$

but in spite of its simplicity it has been successfully applied to soils.

This modification affects only the plastic part of the model, but a similar concept can be used to extend the degradation model to cyclic loading.

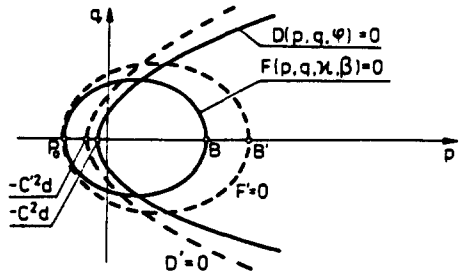

Fig. 5. Yield and degradation surfaces on the p–q plane.

3. COMPARISON WITH EXPERIMENTS

The model has been compared qualitatively with two sets of experimental results by Kotsovos and Newman (1978) and Kupfer *et al.* (1969). They contain a sufficient number of experiments to properly identify material functions, but they are restricted to monotonic conventional triaxial and plane stress tests, respectively. In order to show the model's behaviour for other stress states and paths a qualitative comparison has been made with cubical cell data by Scavuzzo *et al.* (1983). Their experiments cover cyclic behaviour, but do not include any tension results. Other experimental data, which were available two or three years ago, did not provide sufficient information to identify material functions in both tension and compression, except for the strength, which is predicted correctly. The authors prefer not to present comparisons which only represent curve fitting.

It is also necessary to mention that the identification process involves material functions, which have specific physical meaning. However, these functions are approximated by elementary functions, the coefficients of which usually do not have any physical interpretations.

The post-critical parts of the stress–strain response curves shown in the following figures should be treated as extrapolations of the current model behaviour to that range.

3.1. *Axisymmetric tests*

The present model was first applied to describe the confined compression tests made on cylindrical specimens. In these tests two principal stresses are equal and the p–q plane stress and strain measures can be used. The following forms of the yield and the degradation surfaces have been assumed:

$$F(p,q,\kappa,\beta) = q^2 + A(p-P_0)\,[p-B(\kappa,\beta)]$$
$$D(p,q,\phi) = |q|^{3/2} - C(\phi)\,[p-\mathrm{d}C^2(\phi)] \tag{107}$$

The first expression represents an ellipse which intersects the p-axis at the points P_0 and B. The second describes a parabola with a vertex at the point $(-\mathrm{d}C^2, 0)$. They are shown in Fig. 5.

Function ϕ was assumed to depend only on T. It means that only changes of the bulk modulus K are important. The changes of shear modulus G does not affect the degradation. Functions B, C, ϕ were matched according to experimental results and are of the form

$$B(\kappa,\beta) = b_1 \ln(\kappa+b_2) + b_3 \exp(b_4\beta) + b_5$$
$$C(T) = \frac{C_1}{(c_2T^2-1)^{1/2}}$$
$$\phi(T) = \phi_1\left(\frac{T}{T_0}-1\right)^2. \tag{108}$$

Function $C(\phi)$ can be found from $C(T)$ and $\phi(T)$.

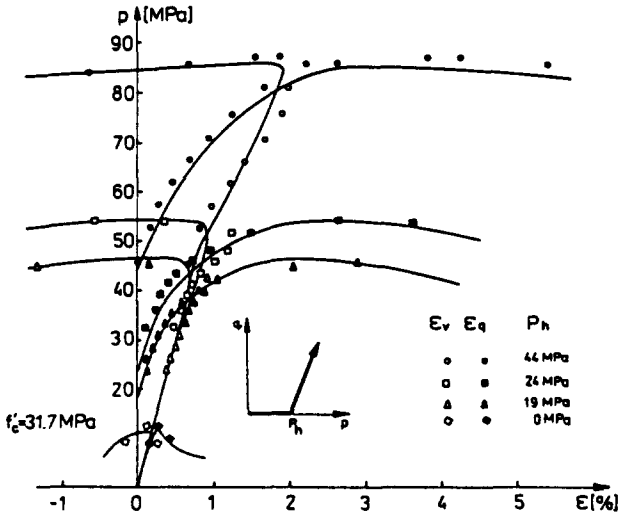

Fig. 6. Confined compression test. Experimental data by Kotsovos and Newman (1978).

The experimental data of Kotsovos and Newman (1978) have been used for identification. The cylindrical samples were subjected to hydrostatic pressure and next compressed axially with a constant lateral pressure. Three types of concrete were used: $f'_c = 31.7$, 46.9, 62.1 MPa. For each of them four different maximum lateral pressures were applied. Figure 6 shows the experimental and theoretical results for the $f'_c = 31.7$ MPa concrete. The results for higher strength concretes are similar and are thus not shown.

3.2. *Biaxial compression*

As the second set of experimental data the biaxial plane stress experiments made by Kupfer *et al.* (1969) were used. The experiments were made on thin square samples subjected to biaxial compression with different principal stress ratios ranging from 1/0 to 1/1. The strength of this concrete was $f'_c = 21.1$ MPa.

Even though these tests are not cyclic, it is better to use the cyclic model to describe the experiments. The main reason is that this model allows for a smooth transition between elastic and plastic regions. The entire stress-strain curve is smooth without any corners. To use this model it was necessary to change slightly the form of the yield surface, and now

$$F(p, q, \kappa, \beta) = q^2 + A[p + f_t B(\kappa, \beta)]\,[p - B(\kappa, \beta)]. \tag{109}$$

Both points on the p-axis move during hardening and when B tends to zero the yield surface tends to the origin. Thus, at the beginning all active surfaces have their characteristic points at the origin. Function $B(\kappa, \beta)$ is of a more general form

$$B(\kappa, \beta) = b_1 \exp(b_2\beta) + b_3(\kappa + b_4)^{b_5} + b_6. \tag{110}$$

The other functions used in this model are of the form described in Section 2.5.

It is also necessary to take into account the influence of the third invariant, since θ is different for uniaxial and biaxial compression states. Without this feature the results would be very inaccurate. For concrete it is well known that the failure surface is dependent on the third invariant. The simplest smooth surface with this influence was proposed by Willam and Warnke (1975). In terms of function g it can be described as follows:

$$g(\theta) = \frac{4(1-e^2)\cos^2\theta + (2e-1)^2}{2(1-e^2)\cos\theta + (2e-1)\,[4(1-e^2)\cos^2\theta + 5e^2 - 4e]^{1/2}} \tag{111}$$

where e is a constant which describes the distance ratio of the failure surface from the hydrostatic axis for $\theta = 0$ and $\pi/3$.

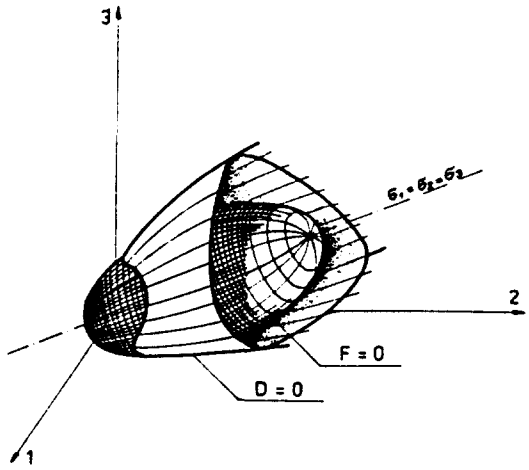

Fig. 7. Yield and degradation surfaces in the principal stress space.

The description of the degradation surface is generalized by the assumption that the power need not be 3/2, and that it also is a material parameter

$$D(p,q,\phi) = |q|^{d_1} - C(\phi)\,[p + d_2 C(\phi)^{1/d_1 - 1}]. \tag{112}$$

This function intersects the q-axis with the same inclination angle independently of the value of ϕ. The $C(\phi)$ function controls the movement of the degradation surface

$$C(\phi) = \frac{c_1}{[c_2(\phi - 1/2)^2 + 1]^{1/2}}. \tag{113}$$

In the pre-critical region the value of C increases and the parabola opens. When ϕ reaches 1/2 the degradation surface becomes the failure surface and next in the post-critical region the parabola closes and the intersection point on the p-axis moves right to zero.

The function ϕ depends on both arguments T and S and is assumed to be defined in terms of a power function

$$\phi(T,S) = \phi_1\{[\phi_2 - (T - T_0)]^{\phi_3} - \phi_2^{\phi_3}\} + \phi_4\{[\phi_5 + (S - S_0)]^{\phi_6} - \phi_5^{\phi_6}\}. \tag{114}$$

Figure 7 shows the shapes of the degradation and yield surfaces in the three-dimensional stress space.

The shape of the failure surface is shown in Figs 8 and 9. It is compared with the experimental data for various types of concrete in a normalized coordinate system. Figures 10–12 show the comparison with the biaxial compression experiments for the principal stress ratios 1/0, 1/0.52, 1/1.

3.3. *Triaxial cyclic tests*

The model described above has also been verified in a qualitative sense for really triaxial tests in which all three principal stresses are different. Such experiments were made at the University of Colorado by Scavuzzo *et al.* (1983). Cubical specimens were tested inside a cubical cell which allows for formation of any compressive triaxial state of stress within cell capacity. The referred paper presents results for many paths in the stress space, but does not contain the simplest types of results which could allow for a fast identification.

Two series of tests have been chosen for verification purposes. In the first, samples were compressed hydrostatically up to a certain pressure value, next unloaded to zero and once again compressed to a higher pressure. In this manner two cycles were performed. Next, the hydrostatic pressure was fixed and cyclic loading was conducted in the deviatoric plane for the constant value of the third angle invariant θ right up to failure. The experimental

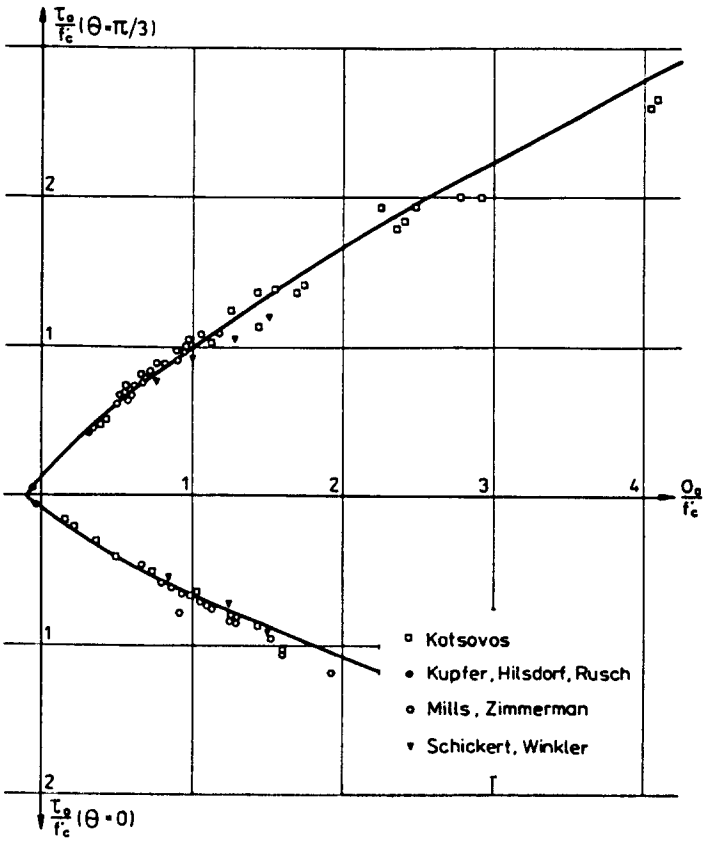

Fig. 8. Failure envelope on the σ_0–τ_0 plane

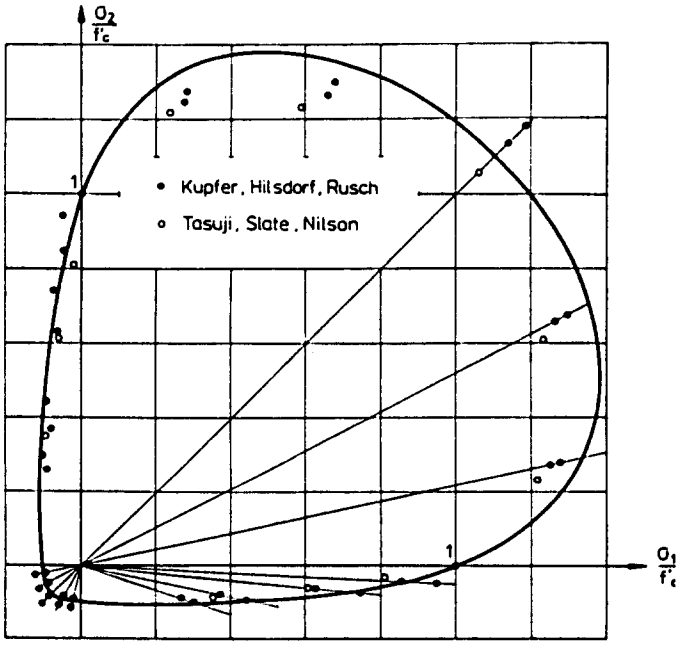

Fig. 9. Biaxial failure envelope.

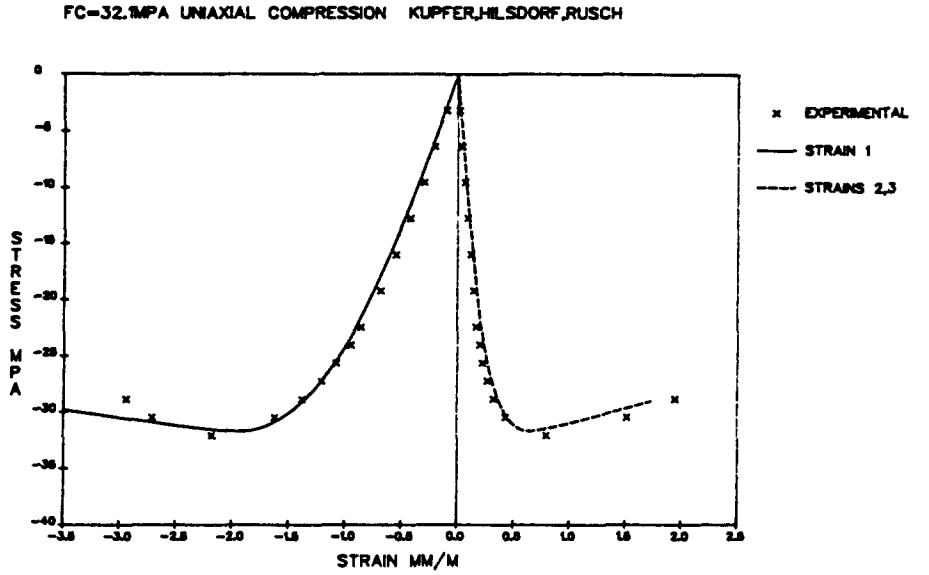

Fig. 10. Uniaxial compression test. Experimental data by Kupfer *et al.* (1969).

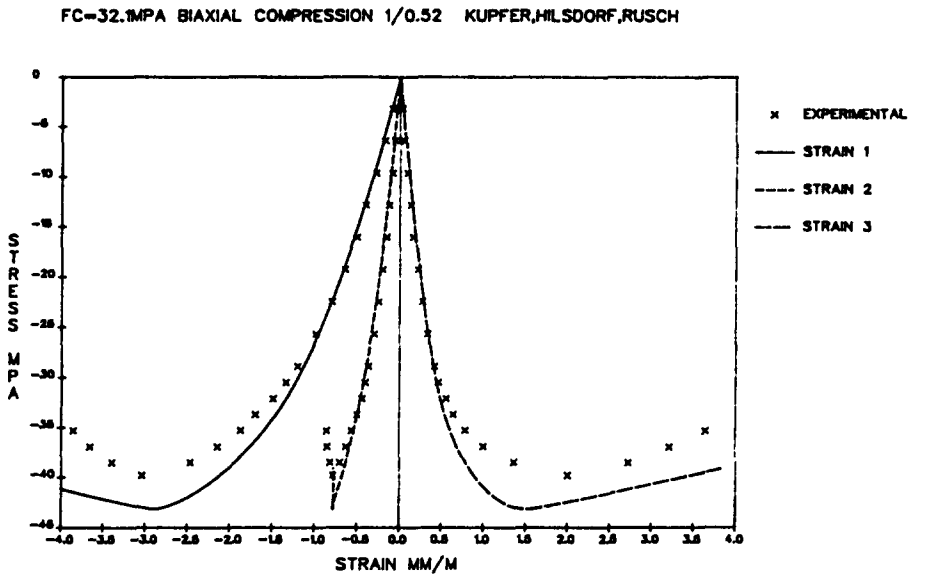

Fig. 11. Biaxial compression $\sigma_1/\phi_2 = 1/0.52$.

results are shown in Fig. 13 and the theoretical prediction for the similar loading path in Fig. 14.

The second series was similar except that the cycles in the deviatoric plane alternate. One of the tests is shown in Figs 15 and 16, and an adequate relationship between experiment and prediction is displayed. The other comparisons within these series are also accurate and thus omitted. The full verification of the model can be found in the report by Klisiński (1984).

4. CONCLUSIONS

For a large number of tests model predictions fit the experiments with a high degree of accuracy. The main limitations are the assumptions of isotropy and the homogeneity of deformation. At the post-critical regime a localization effect is very significant and the macrocracks that develop have a dominant influence on structural behaviour. Further model development should thus be oriented toward these problems and must be considered at the structural level.

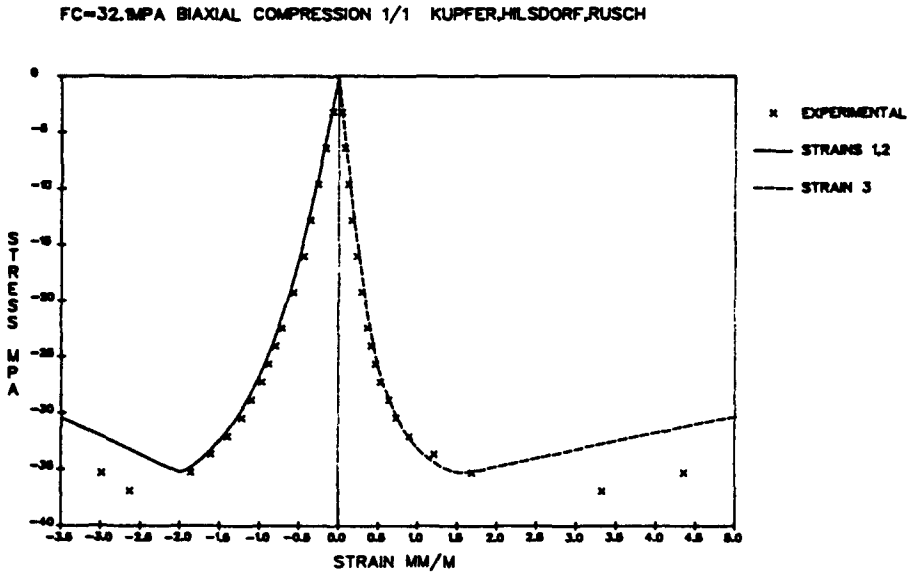

Fig. 12. Biaxial compression $\sigma_1/\sigma_2 = 1/1$.

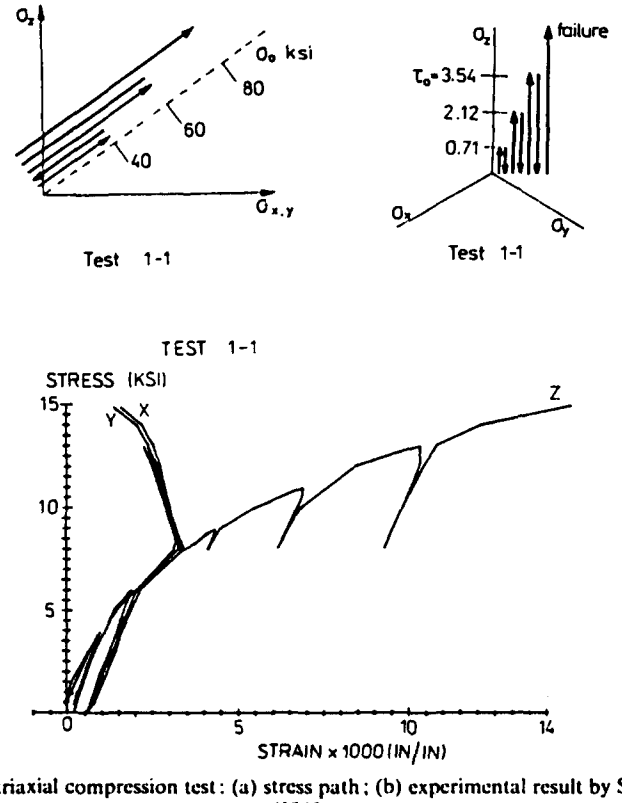

Fig. 13. Cyclic triaxial compression test: (a) stress path; (b) experimental result by Scavuzzo *et al.* (1983).

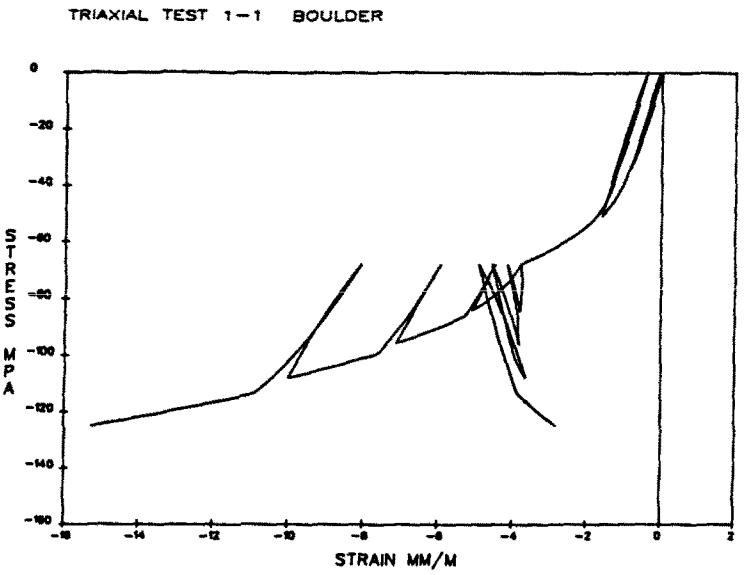

Fig. 14. Qualitative theoretical prediction of test from Fig. 13.

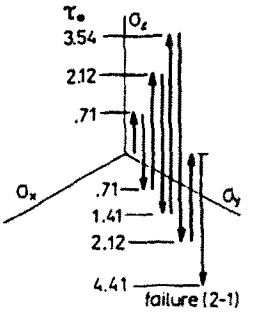

$\sigma_0 = 8$ ksi

TEST 2-1

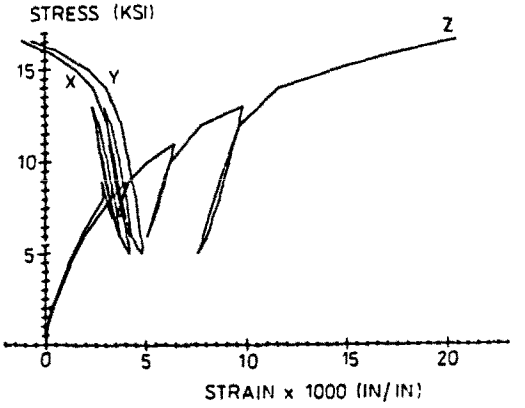

Fig. 15. Cyclic triaxial compression test: (a) stress path; (b) experimental result by Scavuzzo *et al.* (1983).

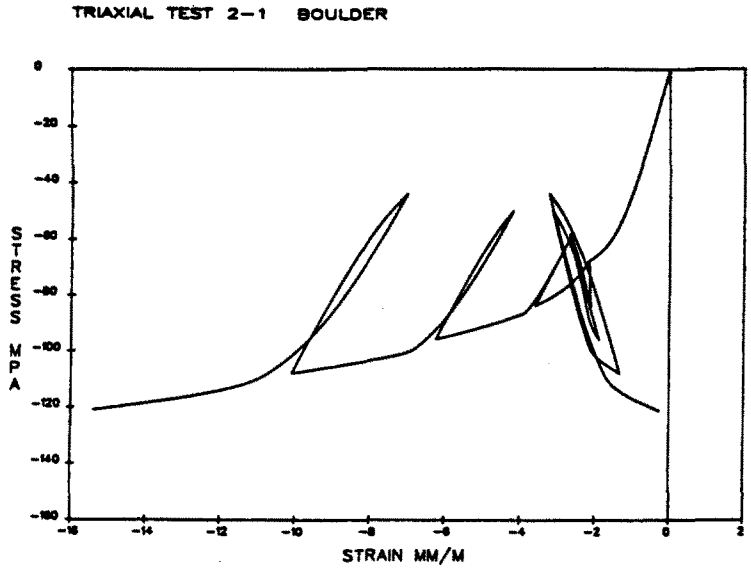

Fig. 16. Qualitative theoretical prediction of test from Fig. 15.

Acknowledgements—The first author gratefully acknowledges the support of the Civil, Environmental and Architectural Engineering Department at the University of Colorado, Boulder, where he spent the academic year 1985–86.

REFERENCES

Bazant, Z. P. and Kim, S. S. (1979). Plastic-fracturing theory for concrete. *J. Engng Mech. Div. ASCE* **105**(EM3), 407–428.

Cedolin, L., Crutzen, Y. R. T. and Dei Poli, S. (1977). Stress–strain relationship and ultimate strength of concrete under triaxial loading conditions. *J. Engng Mech. Div. ASCE* **103**(EM3), 423–439.

Chen, A. C. T. and Chen, W. F. (1975). Constitutive relations for concrete. *J. Engng Mech. Div. ASCE* **101**(EM4), 465–481.

Chen, W. T. (1982). *Plasticity of Concrete*. McGraw-Hill, New York.

Dafalias, Y. F. (1986). Bounding surface plasticity. I: Mathematical foundation and hypoplasticity. *J. Engng Mech. ASCE* **112**(EM9), 966–987.

Dougill, J. W. (1976). On stable, progressively fracturing solids. *J. Appl. Math. Phys. (ZAMP)* **27**, 423–437.

Dougill, J. W., Lau, J. C. and Burt, N. J. (1977). Towards a theoretical model for progressive failure and softening in rock concrete, and similar materials. In *Mechanics in Engineering* (Edited by R. N. Dubey and N. C. Line). University of Waterloo Press.

Dragon, A. and Mróz, Z. (1979). A continuum model for plastic-brittle behavior of rock and concrete. *Int. J. Engng Sci.* **17**, 121–137.

Elwi, A. A. and Murray, D. W. (1979). A 3D hypoelastic concrete constitutive relationship. *J. Engng Mech. Div. ASCE* **105**(EM4), 623–641.

Gerstle, K. H. (1981). Simple formulation of biaxial concrete behavior. *J. Am. Concr. Inst.* **78**(5), 62–68.

Hashiguchi, K. (1980). Constitutive equation of elastoplastic materials with elastic-plastic transition. *J. Appl. Mech. ASME* **47**, 266–272.

Hueckel, T. and Maier, G. (1977). Incremental boundary value problems in the presence of coupling of elastic and plastic deformations: a rock mechanics oriented theory. *Int. J. Solids Structures* **13**, 1–15.

Klisiński, M. (1984). Degradation and plastic deformation of concrete (in Polish). Ph.D. Thesis, IFTR Reports, No. 38.

Kotsovos, M. D. and Newman, J. B. (1978). Generalized stress–strain relations for concrete. *J. Engng Mech. Div. ASCE* **104**(EM4), 845–856.

Krajcinovic, D. and Fonseka, G. B. (1981). The continuous damage theory of brittle materials, Parts I and II. *ASME J. Appl. Mech.* **48**, 809–824.

Kupfer, H., Hilsdorf, H. K. and Rusch, H. (1969). Behavior of concrete under biaxial stresses. *ACI J.* **65**, 8, 656–666.

Lemaitre, J. (1985). A continuous damage mechanics model for ductile fracture. *J. Engng Mater. Technol.* **107**, 83–89.

Liu, T. C. Y., Nilson, A. H. and Slate, F. O. (1972). Biaxial stress–strain relation for concrete. *J. Struct. Div. ASCE* **98**(ST5), 1025–1034.

Mazars, J. (1982). Mechanical damage and fracture of concrete structures. In *Advances in Fracture Research (Fracture 81)*, Vol. 4. Pergamon Press, Oxford.

Mróz, A. and Norris, V. A. (1982). Elasto-plastic and viscoplastic constitutive models with application to cyclic loading for soils. In *Soil Mechanics—Transient and Cyclic Loads* (Edited by G. N. Pande and O. C. Zienkewicz), Chap. 8, pp. 173–217. Wiley, New York.

Mróz, Z. (1973). Mathematical models of inelastic concrete behavior. In *Inelasticity and Nonlinearity in Structural Concrete* (Edited by M. Z. Cohn). University of Waterloo Press.

Mróz, Z. and Pietruszczak, S. (1973). A constitutive model for sand with an anisotropic hardening rule. *Int. J. Numer. Meth. Geom.* **7**, 305–320.
Murray, D. W., Chitnuyanondth, L., Rijnb-Asha, K. Y. and Wong, C. (1979). Concrete plasticity theory for biaxial stress analysis. *J. Engng Mech. Div. ASCE* **105**(EM6), 989–1006.
Ortiz, M. and Popov, E. P. (1982a). Plain concrete as a composite material. *Mech. Mater.* **1**, 139–150.
Ortiz, M. and Popov, E. P. (1982b). A physical model for the inelasticity of concrete. *Proc. R. Soc. London* **A383**, 101.
Ortiz, M. (1985). A constitutive theory for the inelastic behavior of concrete. *Mech. Mater.* **4**, 67–93.
Scavuzzo, R., Stankowski, T., Gerstle, K. H. and Ko, H. Y. (1983). Stress–strain curves for concrete under multiaxial load histories. Dept. of Civil, Env. and Arch. Engng, University of Colorado.
Simo, J. C., Tu, J. W., Taylor, R. L. and Pister, K. S. (1987). *On Strain-based Continuum Damage Models: Formulation and Computational Aspects. Constitutive Laws for Engineering Materials: Theory and Applications* (Edited by C. S. Desai), pp. 233–345. Elsevier, Amsterdam.
Willam, K. J. and Warnke, E. P. (1975). Constitutive model for the triaxial behavior of concrete. *Int. Ass. Bridge Struct. Engng Proc.* **19**, III, 1–30.

APPENDIX

The partial derivatives of p and q are

$$p_{,\sigma_1} = p_{,\sigma_2} = p_{,\sigma_3} = -\tfrac{1}{3}$$

$$q_{,\sigma_1} = \frac{1}{3\rho}[g(\theta)(2s_1 - s_2 - s_3) + m(2J_3[2s_1 - s_2 - s_3] - \rho^2[2s_2s_3 - s_1(s_2 + s_3)])]$$

$$q_{,\sigma_2} = \frac{1}{3\rho}[g(\theta)(2s_2 - s_1 - s_3) + m(2J_3[2s_2 - s_1 - s_3] - \rho^2[2s_1s_3 - s_2(s_1 + s_3)])]$$

$$q_{,\sigma_3} = \frac{1}{3\rho}[g(\theta)(2s_3 - s_1 - s_2) + m(2J_3[2s_3 - s_1 - s_2] - \rho^2[2s_1s_2 - s_3(s_1 + s_2)])]$$

$$p_{,\sigma_x} = p_{,\sigma_y} = p_{,\sigma_z} = -\tfrac{1}{3}$$

$$p_{,\tau_{xy}} = p_{,\tau_{yz}} = p_{,\tau_{zx}} = 0$$

$$q_{,\sigma_x} = \frac{1}{3\rho}[g(\theta)(2s_x - s_y - s_z) + m(2J_3[2s_x - s_y - s_z] - \rho^2[2(s_ys_z - \tau_{yz}^2) - s_x(s_y + s_z) + \tau_{xy}^2 + \tau_{zx}^2])]$$

$$q_{,\sigma_y} = \frac{1}{3\rho}[g(\theta)(2s_y - s_x - s_z) + m(2J_3[2s_y - s_x - s_z] - \rho^2[2(s_xs_z - \tau_{zx}^2) - s_y(s_x + s_z) + \tau_{xy}^2 + \tau_{yz}^2])]$$

$$q_{,\sigma_z} = \frac{1}{3\rho}[g(\theta)(2s_z - s_x - s_y) + m(2J_3[2s_z - s_x - s_y] - \rho^2[2(s_xs_y - \tau_{xy}^2) - s_z(s_x + s_y) + \tau_{yz}^2 + \tau_{zx}^2])]$$

$$q_{,\tau_{xy}} = \frac{2}{\rho}[g(\theta)\tau_{xy} + m(2J_3\tau_{xy} - \rho^2[\tau_{yz}\tau_{zx} - s_z\tau_{xy}])]$$

$$q_{,\tau_{yz}} = \frac{2}{\rho}[g(\theta)\tau_{yz} + m(2J_3\tau_{yz} - \rho^2[\tau_{xy}\tau_{zx} - s_x\tau_{yz}])]$$

$$q_{,\tau_{zx}} = \frac{2}{\rho}[g(\theta)\tau_{zx} + m(2J_3\tau_{zx} - \rho^2[\tau_{xy}\tau_{yz} - s_y\tau_{zx}])]$$

where we denoted

$$m = \frac{2g'(\theta)}{\rho^3\sqrt{\left(1 - \left(\frac{4J_3}{\rho^3}\right)^2\right)}}.$$